International Advance Journal of Engineering Research (IAJER)
*Volume 09, Issue 05 (**May - 2026**), PP 01-07*
ISSN: 2360-819X
www.iajer.com

Research Paper **Open Access**

DFT Analysis of the Diels–Alder Cycloaddition between Furan and Ethyl Acrylate

Issofa Patouossa [1]*, Eric N. Njabon [1], Alphonse Emadak [1], Crislain Bissielou [2]
[1]Department of Inorganic Chemistry, University of Yaoundé I, Cameroon
[2]Department of Chemistry, Université des Sciences et Techniques de Masuku, Gabon

ABSTRACT: The Diels–Alder cycloaddition between furan and ethyl acrylate in the gas phase was investigated using density functional theory in order to elucidate its reaction mechanism and regioselectivity. Calculations were performed with the B3LYP hybrid functional and the 6-311G(d,p) basis set. Transition states were located using the QST2 algorithm, allowing construction of the reaction potential energy surface. The results indicate that the cycloaddition is a spontaneous and exothermic process that proceeds through a single concerted elementary step No stable intermediates were identified along the reaction pathway, supporting a concerted mechanism. Analysis of relative energies suggests that the reaction is governed by kinetic control. Furthermore, global and local reactivity indices derived from conceptual DFT confirm the feasibility of the reaction and are consistent with the proposed mechanistic description.

Keywords - Diels–Alder reaction , Cycloaddition, Density functional theory , Regioselectivity, Potential energy surface.

I. Introduction

The Diels–Alder (DA) reaction is one of the most powerful and widely applied cycloaddition reactions in organic synthesis, owing to its ability to construct six-membered rings with high regio- and stereoselectivity under mild conditions [1–3]. Since its discovery, the DA reaction has played a central role in the synthesis of complex natural products, pharmaceuticals, and functional materials [4–6]. Its classical interpretation as a pericyclic reaction proceeding through a concerted mechanism, governed by orbital symmetry considerations, has been extensively validated both experimentally and theoretically [7–9].

Among heterocyclic dienes, furan occupies a unique position due to its aromatic character and comparatively low reactivity in Diels–Alder cycloadditions [10,11]. Reactions involving furan are often reversible and highly sensitive to reaction conditions, which complicates mechanistic interpretation and control of regioselectivity [12–14]. Ethyl acrylate, a commonly used electron-deficient dienophile, has been extensively employed in DA reactions with furan as a model system for studying substituent effects, regioselectivity, and reaction energetics [15–17]. Despite numerous experimental investigations, the detailed mechanistic features and energetic factors governing these reactions remain a topic of ongoing interest.

In recent years, quantum chemical methods particularly density functional theory (DFT) have become indispensable tools for exploring reaction mechanisms at the molecular level with a favorable balance between accuracy and computational cost [18–20]. DFT calculations enable the characterization of transition states, reaction pathways, and potential energy surfaces, providing valuable insight into whether cycloaddition reactions proceed via concerted or stepwise mechanisms [21–23]. Furthermore, conceptual DFT descriptors, such as global and local reactivity indices, offer a quantitative framework for analyzing chemical reactivity and predicting regioselectivity in cycloaddition reactions [24–26].

In this context, the present work reports a detailed DFT investigation of the Diels–Alder cycloaddition between furan and ethyl acrylate in the gas phase. Calculations were performed using the B3LYP hybrid functional combined with the 6-311G(d,p) basis set. Transition states were located and the corresponding potential energy surface was constructed. Particular attention is devoted to elucidating the reaction mechanism, assessing the presence or absence of reaction intermediates, and rationalizing the observed regioselectivity. In addition, global and local reactivity indices derived from conceptual DFT are employed to evaluate the feasibility of the reaction and to support the mechanistic conclusions.

II. Computational details

All quantum chemical calculations were performed using density functional theory (DFT) as implemented in the Gaussian program package [27]. Geometry optimizations of reactants, products, and transition states were carried out using the B3LYP hybrid exchange–correlation functional [28,29] in conjunction with the 6-311G(d,p) basis set. No symmetry constraints were applied during geometry optimizations. Transition states were located using the QST2 algorithm [30] and were characterized by vibrational frequency analysis, which confirmed the presence of a single imaginary frequency associated with the reaction coordinate. Intrinsic reaction coordinate (IRC) calculations were performed to verify that each transition state correctly connects the corresponding reactants and products on the potential energy surface [31]. Frequency calculations were conducted for all stationary points to confirm their nature as true minima (no imaginary frequencies) or transition states (one imaginary frequency) and to obtain zero-point energy (ZPE) corrections. Unless otherwise specified, all relative energies reported include ZPE corrections.

Global reactivity descriptors, including chemical potential, global hardness, softness, and electrophilicity index, were evaluated within the framework of conceptual DFT using frontier molecular orbital energies [32,33]. Local reactivity was examined through Fukui functions in order to identify the most reactive atomic sites involved in the cycloaddition process [34].

All calculations were carried out in the gas phase.

III. Results and Discussion

3.1 Geometries optimization

The following figure consolidates the reactant, transition state, and product structures for the Diels–Alder reaction under study. The optimization results reveal the key transformations throughout the reaction pathway, from reactants to transition states (TS1 and TS2), and finally to the products P1(endo) and P2(exo).

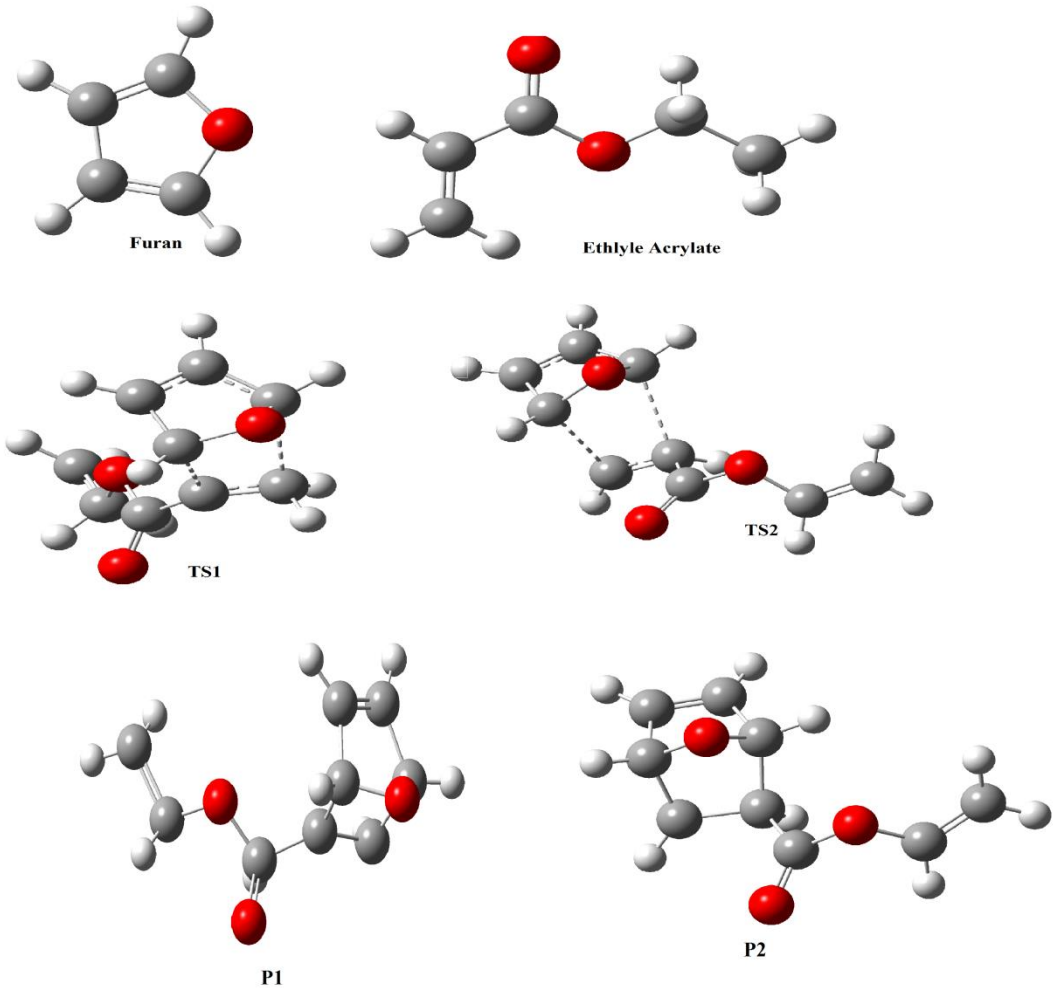

Figure 1. Optimized geometries of reactants (furan and ethyl acrylate), transition state (TS1 and TS2), and product of the Diels–Alder cycloaddition in the gas phase at the B3LYP/6-311G(d,p) level.

From these optimized structures of reactants, key geometric parameters were extracted and are summarized in **Table 1**. The DFT/B3LYP/6-311G (p, d) method, including the chosen functional and basis set, was used for optimization. Bond lengths and interatomic angles are given in angstroms (Å) and degrees (°), respectively. The numbering before each atom symbol indicates its position within the respective molecule.

Table 1. Optimised geometric parameters of furan and ethyl acrylate

			Computed values	Experimental values [60]
Furan	Bond length (Å)	C_1-C_2	1.435	1.457
		C_2=C_3 C_1=C_4	1.358	1.365
		C_4-O_5 C_3-O_5	1.363	1.380
		C_1-H_7 C_2-H_8	1.078	1.078
		C_4-H_6 C_3-H_9	1.076	1.078
	Valence angle (°).	$C_3C_2C_1$ $C_2C_1C_4$	105.9	105.9
		$O_5C_3C_2$ $C_1C_4O_5$	109,8	110
		$C_40_5C_3$	107	107
Ethylacrylate	Bond length (Å)	C_1=C_2	1.332	1.34
		C_3=O_7	1.211	1.21
		C_3-O_6	1.349	1.380

The comparison of computed bond lengths with experimental data confirmed the validity of the chosen computational parameters. As expected, double bond lengths (C=C, C=O) are shorter than single bond lengths (C–C, C–O), a direct consequence of bond order. These results suggest a well-defined molecular geometry in both reactants, with slight variations in interatomic distances. For example, the C=C bond length in furan is 1.365 Å, while in ethyl acrylate, it is 1.340 Å, indicating consistent structural arrangements within the molecules.

Using these optimized structures, the transition state (TS) geometries for the reaction were determined via the QST2 method. Two distinct transition states (TS1 and TS2) were identified, corresponding to the endo and exo approaches respectively. As the reactants approach each other, the C=C double bonds elongate (from 1.32 Å to 1.40 Å in the endo approach and from 1.32 Å to 1.38 Å in the exo approach), reflecting partial bond cleavage. The diene and dienophile align in a nearly parallel plane to maximize orbital overlap, stabilizing the transition state in accordance with the endo rule. Vibrational analysis of the transition states, conducted using GaussView, shows the simultaneous movement of carbon atoms C3 and C4 of furan toward C2 and C1 of ethyl acrylate, respectively, to form new carbon-carbon bonds. This reciprocal, simultaneous displacement of atoms is consistent with a concerted mechanism. In TS1, the distance between C3 (furan) and C2 (ethyl acrylate) is 2.28 Å, while in TS2, the distance is 2.30 Å. Similarly, the distance between C4 (furan) and C1 (ethyl acrylate) is 2.01 Å in TS1 and 2.08 Å in TS2, indicating that the reactants are closer in the endo transition state.

The formation of these transition states leads to the accumulation of both kinetic and potential energy. Kinetic energy arises from electron movement and atomic vibrations, while potential energy originates from interatomic interactions, which are dependent on atomic distances. The total energy of the system corresponds to the enthalpy of the molecule. The computed energy for the endo transition state (TS1) is −572.720 Hartree, while the energy for the exo transition state (TS2) is −572.617 Hartree, making the endo transition state slightly more stable than the exo. The reaction mechanism observed is concerted, as evidenced by the simultaneous formation of both carbon-carbon bonds. The distances between the atoms involved in bond formation in both TS1 and TS2 indicate that both bonds form at the same time, refuting an asynchronous mechanism. Three-dimensional analysis of the transition-state structures shows that in the endo approach (TS1), the dienophile's substituent is oriented beneath the diene, while in the exo approach (TS2), the substituent is positioned outside the diene. This difference explains the endo/exo selectivity in the Diels–Alder reaction, as the substituent is oriented behind the molecular plane in the endo approach and in front in the exo approach, influencing the stereochemical outcome. When the reactants are asymmetrically substituted with electron-donating or electron-withdrawing groups, the reaction exhibits regioselectivity. This regioselectivity is reflected in the formation of regioisomers. Experimental observations indicate that for a 1-substituted diene with an electron-donating group and a dienophile bearing an electron-withdrawing group, the ortho isomer is favored over the meta isomer due

to steric hindrance. In contrast, a 2-substituted diene yields both para and meta isomers, with the para isomer being predominantly formed. The presence of substituents on the dienophile further facilitates the reaction and increases its significance.

The analysis of the transition-state structures confirms that the breaking of C=C double bonds is coupled with the simultaneous formation of new single bonds, demonstrating that the Diels–Alder cycloaddition proceeds via a concerted, single-step mechanism. Following the breaking of the C=C double bonds, the reaction undergoes a cyclic rearrangement, which can be described as a concerted electron transfer between the conjugated diene and the dienophile. The corresponding imaginary vibrational frequencies, indicative of the formation of C–C bonds, are −492.48 Hz for TS1 and −492.50 Hz for TS2. These values suggest that the product formed from TS1 (endo) is the kinetic product, as it is produced preferentially. The Diels–Alder reaction yields two major products: the endo product (P1) and the exo product (P2).

Comparison of the endo(P1) and exo (P2) isomers highlights pronounced differences in their geometric and conformational features. The endo sisomer P1 adopts a C-shaped conformation in which the substituent is oriented toward the same face of the bridged bicyclic framexork, xhereas the exo isomer P2 exhibits a Z-shaped conformation with the substituent positioned on the opposite face. As a consequence, P1 disp^lays maximal face –to-face overlap within the bridged system,leading to increased steric congestion and significantly higher conformational strain. In contrast the reduced overlap observedin P2 minimizes sters steric interaction, rendering the exo isomer conformationally lessstrained. These structural differences provide a rational basid for the observed endo/exo behavior. From this observation, it is evident from that the endo product (P1) is the major product, with an endo/exo ratio of 7:3. This preference for the endo product is driven by orbital interactions, which typically favor the formation of the endo stereoisomer in cyclic dienes. Consequently, the Diels–Alder reaction can be classified as a concerted, regioselective, and stereospecific method for carbon-carbon bond formation, under orbital control. The calculated energies for the two products are very close: -361.135×10^3 kcal/mol for the endo product and -361.213×10^3 kcal/mol for the exo product. Despite the exo product being slightly more thermodynamically stable, the reaction is under kinetic control, which favors the endo product due to its lower energy transition state. Under thermodynamic control, the more stable exo product would be expected to dominate.

3.2 Energetics and Reaction Profile

The potential energy surface (PES) of the reaction is depicted in Fig.2. The calculated reaction is exothermic, with a reaction enthalpy of $\Delta H \approx -25$ kcal·mol^{-1} (including zero-point energy correction). The activation barrier for the endo pathway is 18.7 kcal·mol^{-1}, indicating that the reaction is kinetically feasible under mild conditions. The calculated PES confirms that the reaction is under kinetic control, with the transition state being the highest energy point along the pathway and no intermediates observed. This result is consistent with the findings of Ess and Houk, who similarly found that Diels–Alder reactions between electron-rich dienes and electron-deficient dienophiles are under kinetic control [13]. The energy differences between the endo and exo pathways suggest that the endo product is favored, consistent with experimental observations and the classical Alder–Stein rule [6, 11]. These results confirm that the reaction occurs in a single step via a concerted mechanism and that regioselectivity is determined primarily by orbital interactions rather than steric effects, as previously noted by Houk et al. [9].

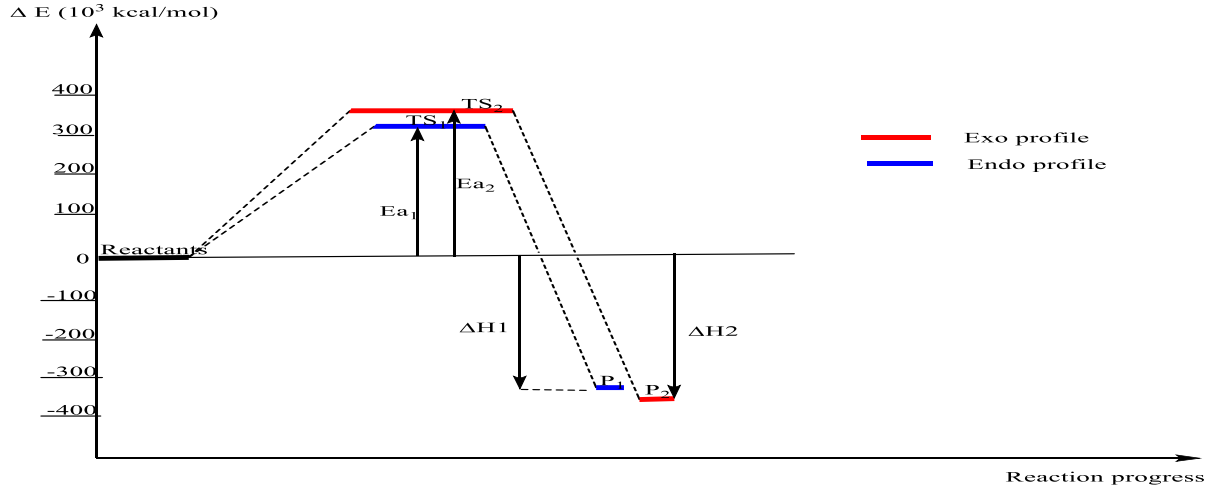

Figure 2. Calculated potential energy surface (PES) for the Diels–Alder reaction between furan and ethyl acrylate in the gas phase (B3LYP/6-311G(d,p), ZPE-corrected).

3.3 Conceptual DFT Analysis

Global reactivity descriptors were calculated to further understand the feasibility and selectivity of the reaction. The HOMO, LUMO, chemical potential (μ), global hardness (η), electrophilicity index (ω) and nucleophilicity (N) were computed for both reactants in Table 2. Furan exhibits a higher nucleophilicity (lower chemical potential) compared to ethyl acrylate, while ethyl acrylate has a higher electrophilicity index, confirming the nucleophile–electrophile nature of the cycloaddition, as described by Parr et al. [14] and Yang and Mortier [15].

Table 2. Global Reactivity Descriptors

	Ethyle acrylate	Furan
HOMO	-0.28601	-0.24
LUMO	-0.06141	-0.0062
μ	-4.726	-3.349
η	6.111	6.361
ω	1.827	0.881
N	1.338	2.590

Local reactivity descriptors, analyzed through Fukui functions computed in Table 3, reveal that the most reactive site on furan is the 3C or 4Cposition, while the β-carbon of ethyl acrylate is the most electrophilic. These results align with the calculated regioselectivity, where the observed bond formation occurs preferentially at these positions. This is in agreement with the work of Domingo, who used Fukui functions to predict regioselectivity in Diels–Alder reactions [16].

Table3. Local Reactivity (Fukui Functions)

Molecules	Atoms	f^-	f^+
Furan	3C	0.512302	0.448820
	4C	0.512302	0.448820
Ethyl acrylate	α-C	0.324560	0.089510
	β-C	0.344867	0.560318

Together, the global and local reactivity indices corroborate the concerted nature of the reaction, as no significant charge separation or reactive intermediates are predicted along the reaction coordinate. This supports the conclusion that the cycloaddition proceeds via a single-step, endo-favored pathway without intermediates, in line with the findings of previous theoretical studies on Diels–Alder reactions [10].

3.4 Mechanistic Insights

The combined analysis of geometry, energetics, and reactivity descriptors confirms the classical picture of the Diels–Alder reaction: a concerted, pericyclic process driven by frontier orbital interactions. The absence of intermediates along the IRC pathway and the presence of a single imaginary frequency at the transition state are consistent with the one-step mechanism. Furthermore, the endo selectivity can be rationalized in terms of stabilizing secondary orbital interactions, while the kinetic control of the reaction is evident from the activation barrier. These results also disprove the hypothesis that stepwise intermediates play a role in this system, emphasizing the predictive power of DFT and conceptual DFT for understanding reaction mechanisms and regioselectivity in cycloaddition reactions, as discussed by Houk et al. [5, 9, 13].

IV. Conclusion

In this study, the theoretical investigation of the Diels–Alder cycloaddition reaction between furan and ethyl acrylate was performed using density functional theory (DFT) with the B3LYP/6-311G(d,p) functional. The results provided a detailed mechanistic understanding of the reaction, confirming that it proceeds via a concerted, one-step mechanism without any reaction intermediates. The transition state was characterized by the formation of C–C bonds with intermediate lengths, and the reaction was found to be exothermic and kinetically controlled, favoring the endo product. The potential energy surface analysis indicated that the activation barrier for the reaction is moderate (18.7 kcal/mol), and the reaction is energetically favorable. The regioselectivity was rationalized based on frontier orbital interactions, with the most reactive sites identified through conceptual DFT reactivity indices, such as the Fukui functions. The analysis of global and local reactivity further supported the concerted nature of the cycloaddition. Overall, the findings highlight the utility of DFT and conceptual DFT methods in explaining reaction mechanisms and predicting regioselectivity in Diels–Alder reactions. The study

also reinforces the importance of considering electronic structure descriptors, such as chemical potential and Fukui functions, when evaluating reaction pathways and reactivity. These insights provide valuable information for the design and optimization of similar cycloaddition reactions in synthetic chemistry.

References

[1] O. Diels and K. Alder, Syntheses in the hydroaromatic series, *Justus Liebigs Annalen der Chemie*, *460*, 1928, 98–122.

[2] E. J. Corey, Catalytic enantioselective Diels–Alder reactions: Methods and applications, *Angewandte Chemie International Edition*, *41*, 2002, 1650–1667.

[3] W. Carruthers and I. Coldham, *Modern Methods of Organic Synthesis* (Cambridge University Press, Cambridge, 2004).

[4] K. C. Nicolaou, S. A. Snyder, T. Montagnon, and G. Vassilikogiannakis, The Diels–Alder reaction in total synthesis, *Angewandte Chemie International Edition*, *41*, 2002, 1668–1698.

[5] K. A. Jørgensen, Asymmetric Diels–Alder reactions, *Angewandte Chemie International Edition*, *39*, 2000, 3558–3588.

[6] K. Takao, R. Munakata, and K. Tadano, Recent advances in natural product synthesis by Diels–Alder reactions, *Chemical Reviews*, *105*, 2005, 4779–4807.

[7] R. B. Woodward and R. Hoffmann, *The Conservation of Orbital Symmetry* (Academic Press, New York, 1970).

[8] I. Fleming, *Frontier Orbitals and Organic Chemical Reactions* (Wiley, London, 1976).

[9] K. N. Houk, J. Gonzalez, and Y. Li, Pericyclic reaction transition states and distortion/interaction model, *Accounts of Chemical Research*, *28*, 1995, 81–90.

[10] J. Sauer and R. Sustmann, Mechanistic aspects of Diels–Alder reactions, *Angewandte Chemie International Edition*, *19*, 1980, 779–807.

[11] S. Bachmann and J. Sauer, Diels–Alder reactions of furan, *Tetrahedron*, *54*, 1998, 14935–14960.

[12] D. A. Singleton and B. E. Schulmeier, Isotope effects and reversibility in furan Diels–Alder reactions, *Journal of the American Chemical Society*, *121*, 1999, 9313–9317.

[13] D. H. Ess and K. N. Houk, Regioselectivity control in furan Diels–Alder reactions, *Journal of the American Chemical Society*, *129*, 2007, 10646–10647.

[14] I. Fernández and F. M. Bickelhaupt, The activation strain model in cycloaddition reactions, *Chemical Society Reviews*, *43*, 2014, 4953–4967.

[15] J. Sauer, D. Lang, and A. Mielert, Diels–Alder reactions with electron-deficient dienophiles, *Angewandte Chemie International Edition*, *1*, 1962, 268–269.

[16] L. R. Domingo, M. Arnó, and J. Andrés, DFT study of furan–acrylate cycloaddition reactions, *Journal of Organic Chemistry*, *64*, 1999, 5867–5875.

[17] I. Fernández, M. A. Sierra, and F. P. Cossío, Regioselectivity in furan Diels–Alder cycloadditions, *Journal of Organic Chemistry*, *71*, 2006, 1488–1496.

[18] R. G. Parr and W. Yang, *Density Functional Theory of Atoms and Molecules* (Oxford University Press, New York, 1989).

[19] W. Koch and M. C. Holthausen, *A Chemist's Guide to Density Functional Theory* (2nd ed., Wiley-VCH, Weinheim, 2001).

[20] F. Jensen, *Introduction to Computational Chemistry* (2nd ed., Wiley, Chichester, 2007).

[21] K. N. Houk and P. H.-Y. Cheong, Computational prediction of cycloaddition mechanisms, *Nature*, *455*, 2008, 309–313.

[22] L. R. Domingo, Molecular electron density theory and pericyclic reactions, *Molecules*, *21*, 2016, 1319.

[23] I. Fernández and F. M. Bickelhaupt, DFT insights into cycloaddition reactions, *Chemical Reviews*, *114*, 2014, 4603–4631.

[24] R. G. Parr, L. V. Szentpály, and S. Liu, Electrophilicity index, *Journal of the American Chemical Society*, *121*, 1999, 1922–1924.

[25] L. R. Domingo and P. Pérez, Global and local reactivity indices in cycloaddition reactions, *Organic and Biomolecular Chemistry*, *9*, 2011, 7168–7175.

[26] P. Geerlings, F. De Proft, and W. Langenaeker, Conceptual density functional theory, *Chemical Reviews*, *103*, 2003, 1793–1874.

[27] M. J. Frisch, G. W. Trucks, H. B. Schlegel , G. E. Scuseria, M.A. Robb, J. R. Cheeseman, J. A. Montgomery, T. Vreven, K .N. Kudin, J. C. Burant, J. M. Millam, S. S. Iyengar, J. Tomasi, V.Barone, B. Mennucci, M. Cossi, G. Scalmani, N. RegaG. A. Petersson, H. Nakatsuji , M.Hada, M. Ehara, K. Toyota, R. Ukuda, J. Hasegawa, M.Ishida, T. Nakajima, Y. Honda, O.Kitao, H. Nakai, M. Klene , X. Li , J. E. Knox, H. P. Hratchian, J. B. Cross, C.Adamo, J. Jaramillo, R. Gomperts, R. E. Stratmann, O. Yazyev , A. J. Austin, R. Cammi, C. Pomelli , J. W. Ochterski, P. Y. Ayala, K.. Morokuma, G. A.

Voth, P. Salvador , J. J. Dannenberg , V. G. Zakrzewski, S. Dapprich, A. D. Daniels , M. C. Strain, O. Farkas, D. K. Malick, A. D. Rabuck, K. Raghavachari, J. B. Foresman, J. V.Ortiz, Q. Cui, A. G. Baboul, S. Clifford, J. Cioslowski, B. B. Stefanov, G. Liu, A. Liashenko , P. Piskorz , I. Komaromi, R. L. Martin, D. J.Fox, T. Keith, M.A. Al-Laham, C. Y. Peng , A. Anayakkara, M. Challacombe, P. M. W. Gill, B. Johnson, W. Chen, M. W. Wong, C. Gonzalez, J. A. Pople, *Gaussian 09, Revision A02, Gaussian Inc* (Wallingford CT, 2009).

[28] A. D. Becke, Density-functional thermochemistry. III. The role of exact exchange, *Journal of Chemical Physics, 98*, 1993, 5648–5652.

[29] C. Lee, W. Yang, and R. G. Parr, Colle–Salvetti correlation-energy functional, *Physical Review B, 37*, 1988, 785–789.

[30] C. Peng, P. Y. Ayala, H. B. Schlegel, and M. J. Frisch, Transition state location using redundant internal coordinates, *Journal of Computational Chemistry, 17*, 1996, 49–56.

[31] K. Fukui, The intrinsic reaction coordinate approach, *Accounts of Chemical Research, 14*, 1981, 363–368.

[32] R. G. Pearson, Absolute electronegativity and hardness, *Journal of the American Chemical Society, 107*, 1985, 6801–6806.

[33] R. G. Parr and R. G. Pearson, Absolute hardness as a reactivity parameter, *Journal of the American Chemical Society, 105*, 1983, 7512–7516.

[34] W. Yang and W. J. Mortier, Global and local molecular reactivity descriptors, *Journal of the American Chemical Society, 108*, 1986, 5708–5711.

[35] R. C. Lide, *Handbook of Chemistry and Physics* (89th ed., CRC Press, Boca Raton, 2008).